ATF6 Regulates Cardiac Hypertrophy by Transcriptional Induction of the mTORC1 Activator, Rheb

Erik A. Blackwood, Christoph Hofmann, Michelle Santo Domingo, Alina S. Bilal, Anup Sarakki, Winston Stauffer, Adrian Arrieta, Donna J. Thuerauf, Fred W. Kolkhorst, Oliver J. Müller, Tobias Jakobi, Christoph Dieterich, Hugo A. Katus, Shirin Doroudgar, Christopher C. Glembotski

Rationale: **Endoplasmic reticulum (ER) stress dysregulates ER proteostasis, which activates the transcription factor, ATF6 (activating transcription factor 6α), an inducer of genes that enhance protein folding and restore ER proteostasis. Because of increased protein synthesis, it is possible that protein folding and ER proteostasis are challenged during cardiac myocyte growth. However, it is not known whether ATF6 is activated, and if so, what its function is during hypertrophic growth of cardiac myocytes.**

Objective: **To examine the activity and function of ATF6 during cardiac hypertrophy.**

Methods and Results: **We found that ER stress and ATF6 were activated and ATF6 target genes were induced in mice subjected to an acute model of transverse aortic constriction, or to free-wheel exercise, both of which promote adaptive cardiac myocyte hypertrophy with preserved cardiac function. Cardiac myocyte-specific deletion of *Atf6* (ATF6 cKO [conditional knockout]) blunted transverse aortic constriction and exercise-induced cardiac myocyte hypertrophy and impaired cardiac function, demonstrating a role for ATF6 in compensatory myocyte growth. Transcript profiling and chromatin immunoprecipitation identified *RHEB* (Ras homologue enriched in brain) as an ATF6 target gene in the heart. RHEB is an activator of mTORC1 (mammalian/mechanistic target of rapamycin complex 1), a major inducer of protein synthesis and subsequent cell growth. Both transverse aortic constriction and exercise upregulated *RHEB*, activated mTORC1, and induced cardiac hypertrophy in wild type mouse hearts but not in ATF6 cKO hearts. Mechanistically, knockdown of ATF6 in neonatal rat ventricular myocytes blocked phenylephrine- and IGF1 (insulin-like growth factor 1)-mediated *RHEB* induction, mTORC1 activation, and myocyte growth, all of which were restored by ectopic RHEB expression. Moreover, adeno-associated virus 9-*RHEB* restored cardiac growth to ATF6 cKO mice subjected to transverse aortic constriction. Finally, ATF6 induced *RHEB* in response to growth factors, but not in response to other activators of ATF6 that do not induce growth, indicating that ATF6 target gene induction is stress specific.**

Conclusions: **Compensatory cardiac hypertrophy activates ER stress and ATF6, which induces *RHEB* and activates mTORC1. Thus, ATF6 is a previously unrecognized link between growth stimuli and mTORC1-mediated cardiac growth. (*Circ Res*. 2019;124:79-93. DOI: 10.1161/CIRCRESAHA.118.313854.)**

Key Words: ATF6 ■ cardiac hypertrophy ■ ER stress ■ mTORC1 ■ proteostasis

Protein homeostasis, or proteostasis, involves the coordination of protein synthesis and folding to ensure proteome integrity and vital cell function.[1] In cardiac myocytes, the endoplasmic reticulum (ER) is a major site of synthesis of proteins that are critical for proper function of the heart, including many calcium-handling proteins, receptors, and secreted proteins, such as hormones, stem cell homing factors, and growth factors.[2,3] Therefore, ER proteostasis maintains the integrity of the cardiac myocyte proteome and thus cardiac contractility. Increased protein synthesis in growing cardiac myocytes must be balanced by increased protein folding to avoid the accumulation of toxic, misfolded

Editorial, see p 9
In This Issue, see p 2
Meet the First Author, see p 3

Original received August 5, 2018; accepted October 17, 2018. In September 2018, the average time from submission to first decision for all original research papers submitted to *Circulation Research* was 14.06 days.

From the Department of Biology, San Diego State University Heart Institute, San Diego State University, CA (E.A.B., C.H., M.S.D., A.S.B., A.S., W.S., A.A., D.J.T., F.W.K., C.C.G.); Department of Cardiology, Angiology, and Pneumology, University Hospital Heidelberg, Germany (C.H., O.J.M., H.A.K., S.D.); German Centre for Cardiovascular Research, Partner Site Heidelberg (C.H., O.J.M., T.J., C.D., H.A.K., S.D.); Department of Internal Medicine III, University of Kiel, Germany, and German Centre for Cardiovascular Research, Partner Site Hamburg/Kiel/Lübeck, Germany (O.J.M.); and Section of Bioinformatics and Systems Cardiology, Department of Internal Medicine III, University Hospital Heidelberg, Germany (T.J., C.D.).

The online-only Data Supplement is available with this article at https://www.ahajournals.org/doi/suppl/10.1161/CIRCRESAHA.118.313854.

Correspondence to Christopher C. Glembotski, PhD, Department of Biology, San Diego State University (SDSU) Heart Institute, San Diego State University, 5500 Campanile Dr, San Diego, CA 92182. Email cglembotski@mail.sdsu.edu

Novelty and Significance

What Is Known?

- Cardiac myocytes in the heart exhibit adaptive hypertrophic growth in response to pathological and physiological conditions, both of which activate mTORC1 (mammalian/mechanistic target of rapamycin complex 1) signaling and increase protein synthesis—critical drivers of cardiac growth.
- Increased protein synthesis places demands on the protein-folding machinery in cardiac myocytes, leading to some protein misfolding, which activates the transcription factor, ATF6 (activating transcription factor 6α), which regulates a gene program that fortifies cellular protein-folding capacity.

What New Information Does This Article Contribute?

- Selective deletion of ATF6 in cardiac myocytes of mice impaired mTORC1 signaling, protein synthesis, and cardiac hypertrophy, demonstrating that ATF6 is required for heart growth.
- Selective activation of ATF6 in mouse hearts induced *RHEB* (ras homologue enriched in brain)—a required activator of mTORC1 and protein synthesis—identifying ATF6 as a previously unrecognized link between pathological and physiological growth stimuli and mTORC1-mediated increases in protein synthesis, protein folding, and cardiac growth.

Endoplasmic reticulum (ER) stress impairs ER protein folding, which activates the transcription factor, ATF6—an inducer of genes that restore ER protein folding. We hypothesized that increased protein synthesis during cardiac hypertrophy might challenge ER protein folding, leading to ATF6 activation. We found that ER stress and ATF6 were activated in mice subjected to pathological and physiological growth conditions that promote adaptive cardiac myocyte hypertrophy. Cardiac myocyte-specific deletion of ATF6 blunted adaptive cardiac myocyte hypertrophy, whereas ectopic expression of ATF6 enhanced the hypertrophic response. Here, ATF6 promoted the induction of *RHEB*—an obligate activator of mTORC1, a known regulator of protein synthesis and cellular growth. Ectopic expression of *RHEB* restored cardiac growth to ATF6 cKO (conditional knockout) mice. ATF6 induced *RHEB* in response to growth factors, but not in response to other activators of ATF6 that do not induce growth, indicating that ATF6 target gene induction is stress specific. Thus, ATF6 is a newly identified, essential member of mTORC1-mediated growth signaling in the heart. Moreover, because ATF6 is ubiquitously expressed, our findings underscore the potential widespread importance of this new ATF6-Rheb-mTORC1 growth signaling axis in noncardiac cells and tissues in addition to the heart.

Nonstandard Abbreviations and Acronyms

4E-BP1	4E-binding protein 1
AAV	adeno-associated virus
ATF6	activating transcription factor 6α
cKO	conditional knockout
ER	endoplasmic reticulum
ERSE	endoplasmic reticulum stress response element
GAP	GTPase-activating protein
IGF1	insulin-like growth factor 1
mTORC1	mammalian/mechanistic target of rapamycin complex 1
NRVM	neonatal rat ventricular myocyte
Rheb	Ras homologue enriched in brain
sI/R	simulated ischemia/reperfusion
TAC	transverse aortic constriction
UPR	unfolded protein response

proteins; thus, growth poses a potential challenge to cardiac myocyte proteostasis.[4] However, the molecular mechanisms underlying the maintenance of ER proteostasis during cardiac myocyte growth are not well understood.

ER proteostasis is controlled in all mammalian cells by several ER transmembrane sensors of protein misfolding, including the adaptive transcription factor, ATF6 (activating transcription factor 6α).[5] When protein synthesis surpasses the capacity of the protein-folding machinery, increases in misfolded proteins cause the translocation of the ER transmembrane, 670-amino acid, 90 kD form of ATF6, to the Golgi, where it is clipped, liberating an N-terminal fragment that serves as a transcription factor. This 50-kD active form of ATF6 regulates a gene program that is responsible for the expression of numerous proteins that enhance ER protein folding, which adaptively restores the balance between protein synthesis and folding.[6,7] Thus, nodal proteostasis regulators, such as ATF6, that sense and maintain this balance could play important roles in optimizing cardiac myocyte growth; however, neither the activation nor the function of ATF6 in the setting of hypertrophic growth of the heart has been examined. Accordingly, here, we studied the effects of *Atf6* deletion in mouse hearts and in cultured cardiac myocytes during physiologically relevant maneuvers known to promote compensatory cardiac hypertrophy in either a concentric (pressure overload)[8] or eccentric (exercise)[9] manner, positing that the absence of ATF6 would imbalance proteostasis, which would be maladaptive.

Both growth maneuvers activated ATF6, and *Atf6* deletion was maladaptive, as evidenced by impaired cardiac function. However, surprisingly, cardiac myocyte growth was also impaired on *Atf6* deletion. This was unexpected because *Atf6* is not known to be required for cardiac myocyte growth. Further mechanistic studies showed that ATF6 is activated as a result of the increased demands placed on the ER protein folding machinery during growth-related increases in protein synthesis. Moreover, we found that *Atf6* serves a previously unrecognized role as a molecular link between growth stimuli ER stress and activation of mTORC1 (mammalian/mechanistic target of rapamycin complex 1), a major promoter of protein synthesis and consequent growth of cardiac myocytes.[10–15] Two conditions need to be met for mTORC1 to be activated: (1) in response to a growth stimulus, mTORC1 needs to translocate to organelles, such as lysosomes,[16] where it encounters the small GTPase activator of mTORC1, Rheb (Ras homologue enriched in brain),[17] and (2) Rheb must be active and present in sufficient quantities.[18] In terms of Rheb activation, it is known that growth stimuli lead to the phosphorylation and, thus, inhibition

of the Rheb GAP (GTPase-activating protein), TSC1/TSC2 (tuberous sclerosis gene product-1 and -2),[19] which increases the GTP-loading state and, thus, the activity of Rheb. However, the molecular mechanisms underlying the *Rheb* gene expression are less well understood. Here, we showed, for the first time, that ATF6 is an inducer of *RHEB*, and in this way, ATF6 coordinates protein synthesis and protein folding, ensuring the adaptive maintenance of proteostasis in growing cardiac myocytes. Thus, ATF6 is a newly identified and essential member of mTORC1 growth signaling in cardiac myocytes in the heart.

Methods

All supporting data are available within the article. Further details on the Methods can be found in the Online Data Supplement.

Laboratory Animals

The research reported in this article has been reviewed and approved by the San Diego State University Institutional Animal Care and Use Committee, and it conforms to the Guide for the Care and Use of Laboratory Animals published by the National Research Council.

ATF6 Floxed Mice

Atf6α$^{fl/fl}$ mice used in this study were generated by Dr Gokhan S. Hotamisligil.[20] All of the mice used in this study were 10-week-old males.

Statistics

Unless otherwise stated, values shown are mean±SEM, and statistical treatments are either a *t* test or a 1-way ANOVA followed by Newman-Keuls post hoc analysis.

Results

ATF6 Is Required for Cardiac Myocyte Hypertrophy in Response to Pressure Overload

To examine the role of *Atf6* in cardiac myocytes on heart growth, we generated an ATF6 cKO (conditional knockout) mouse line by injecting *Atf6*$^{fl/fl}$ mice with a recombinant adeno-associated virus (AAV) 9 that encodes *Cre* under the control of the cardiac troponin T promoter (Figure 1A). Compared with *Atf6*$^{fl/fl}$ injected with AAV9-Con (Con), injection with AAV9-CRE effectively reduced *Atf6* mRNA in cardiac myocytes isolated from *Atf6*$^{fl/fl}$ mice but not noncardiac myocytes or liver (Figure 1B). *Atf6*$^{fl/fl}$ mice injected with AAV9-Con or AAV9-CRE (ATF6 cKO) were subjected to transverse aortic constriction (TAC) and examined 7 days later, when hypertrophic growth is maximal[21] and structural remodeling is compensatory.[22,23] TAC activated ATF6 in Con mouse hearts, as evidenced by increased levels of the active, 50 kD form of ATF6 (Figure 1C). This was unexpected because ATF6 is not known to be activated in cardiac myocytes by any growth stimulus. Coordinate with ATF6 activation, TAC increased expression of numerous canonical ATF6 target genes (Figure 1C and 1D; Online Figure IA). As expected, ATF6 was undetectable in ATF6 cKO mouse hearts (Figure 1C and 1D). TAC increased Con mouse heart weights, but, surprisingly, this growth effect was significantly blunted in ATF6 cKO mouse hearts (Figure 1E). TAC increased *Nppa* and *Nppb* expression to similar extents in both Con and ATF6 cKO mice, whereas the induction of *Myh7* and *Col1a1* was slightly greater in the ATF6 cKO mice (Figure 1F). This, coupled with the decrease in *Atp2a2* (ie, *SERCA2a* in ATF6 cKO mice), suggests a blunted compensatory response in the absence of ATF6. In Con mouse hearts, cardiac function, including fractional shortening, was preserved, whereas chamber dimensions were unchanged after TAC (Figure 1G; Online Table I) and cardiac myocyte size was increased (Figure 1H), consistent with the compensatory nature of cardiac hypertrophy in mice at this time after pressure overload.[24] However, in contrast to Con, in ATF6 cKO mice subjected to TAC, myocyte size was decreased compared with Con (Figure 1H), and fractional shortening was impaired (Figure 1G) with increased chamber dimensions, such as left ventricular end diastolic volume and left ventricular end systolic volume, despite high-frequency Doppler measurements between right and left carotid arteries demonstrating consistent and identical pressure overload in TAC-operated Con and ATF6 cKO mice (Online Table I). Along with increased plasma levels of cTnI (cardiac troponin I; Online Figure IB), these results are consistent with the initial stages of chamber dilation, as well as myocardial damage and decompensation in the ATF6 cKO mice. Thus, ATF6 is activated by pressure overload and is required for hypertrophy.

ATF6 Is Required for Cardiac Myocyte Hypertrophy in Response to Exercise

To assess the breadth of the impact of ATF6 on heart growth, we examined the effects of cardiac myocyte-specific ATF6 deletion in mice subjected to free-wheel exercise[25,26] (Figure 2A). Similar to TAC, exercise surprisingly activated ATF6 and induced ATF6 target genes in Con but not in ATF6 cKO mice (Figure 2B and 2C). As expected, compared with Con sedentary mice, Con mice subjected to exercise exhibited increased heart weights and left ventricle wall thickness, as well as myocyte size (Figure 2D and 2F; Online Table II). Whereas *Nppa* and *Nppb* were mildly increased, *Atp2a2* was robustly increased by exercise in Con mouse hearts, and there was no change in *Myh7* or *Col1a1* (Figure 2E); this gene profile is typical of adaptive cardiac hypertrophy in exercising mice.[24,27] In contrast to Con, in ATF6 cKO mice subjected to exercise, there was no change in heart weights or left ventricular wall thickness (Figure 2D; Online Table II), moderated increases in myocyte size (Figure 2F), and reduced induction of ATF6 target genes (Figure 2C). Compared with exercised Con mice, exercised ATF6 cKO mice showed no increase in *Nppa*, and neither Con nor ATF6 cKO mice showed significant changes in *Nppb* or *Myh7*. Importantly, whereas Con mice exhibited decreased *Col1a1* and increased *Atp2a2* after exercise, which are beneficial genetic changes typical of this maneuver, the ATF6 cKO mice failed to adapt and had increased *Col1a1* and no change in *Atp2a2* (Figure 2E). Thus, ATF6 is activated by exercise and is required for compensatory hypertrophy in this exercise model.

Rheb Is an ATF6-Inducible Gene in the Heart

Since there are no known *Atf6*-inducible genes that are required for cardiac myocyte growth; we turned to transcript profiling for clues to the identities of such genes. RNA sequencing of the hearts of our previously published transgenic mice that express activated ATF6[28] (Online Table III) revealed that ATF6 induced 51 genes in the gene ontology category, small GTPase mediated signal transduction; this category includes the Ras-related small GTPase, *RHEB* (Figure 3A; Online Figure IIA). Rheb is required for activation of mTORC1, however, only in

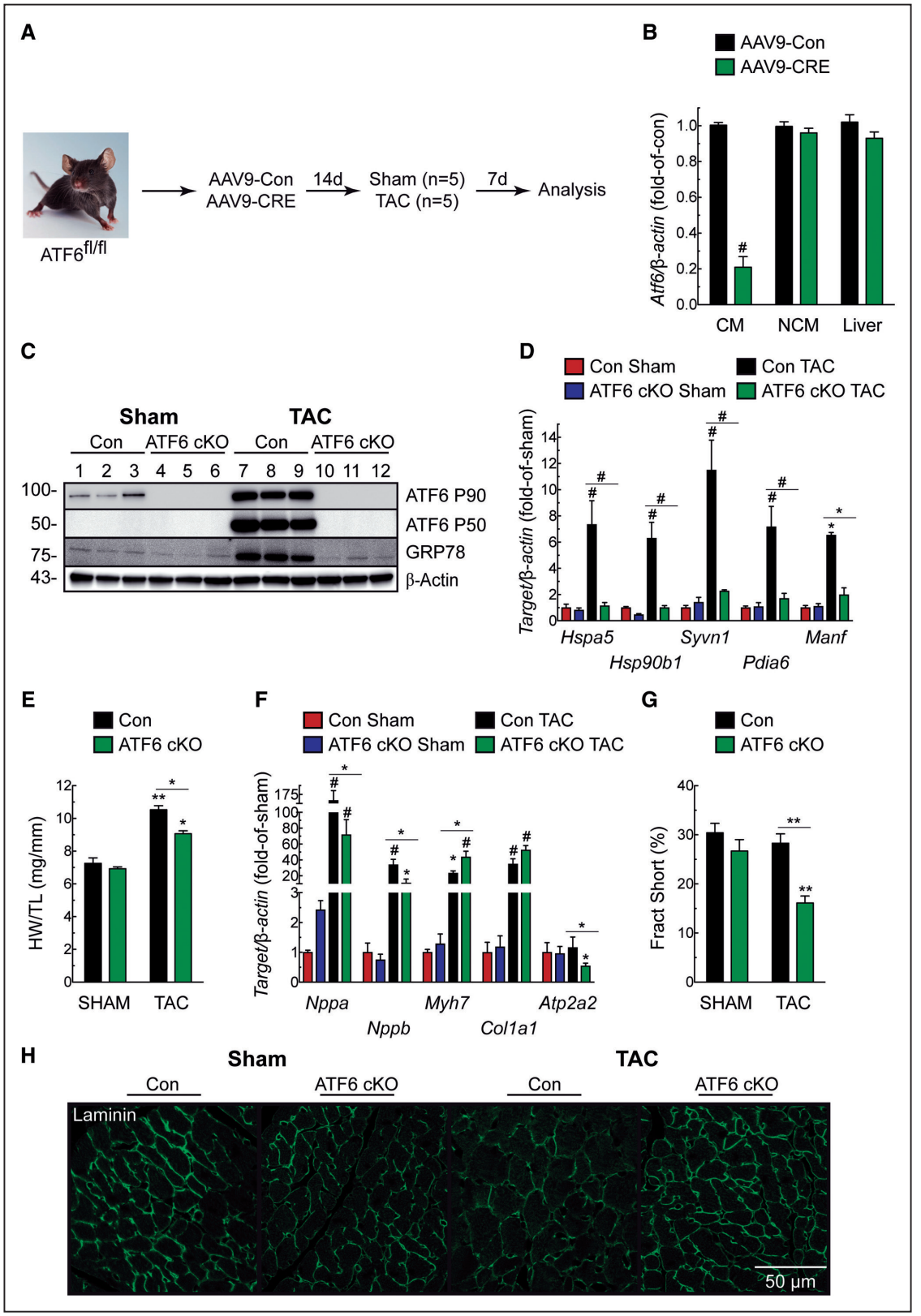

Figure 1. Effect of cardiac myocyte-specific *ATF6* (activating transcription factor 6α) gene deletion in hearts of mice subjected to transverse aortic constriction (TAC). A, Protocol for adeno-associated virus (AAV) 9 administration to ATF6$^{fl/fl}$ mice and TAC. **B**, ATF6 mRNA levels determined by quantitative real-time polymerase chain reaction (qRT-PCR) on isolated cardiac myocyte (CM), noncardiac myocyte (NCM), and liver extracts from ATF6$^{fl/fl}$ mice injected with AAV9-Con (Con) or AAV9-CRE (ie, ATF6 cKO [conditional knockout]); n=3. **C**, Immunoblot of left ventricular extracts from Con or ATF6 cKO mice. **D**, mRNA for ATF6 target genes determined by qRT-PCR. **E**, Heart weight/tibia length (HW/TL). **F**, mRNA levels for fetal genes determined by qRT-PCR. **G**, Fractional shortening (%), determined by echocardiography (Online Table I). **H**, Confocal immunocytofluorescence microscopy analysis of mouse heart sections for laminin (green). Data are mean±SEM. **P*≤0.05, ***P*≤0.01, #*P*≤0.001 different from Con Sham or from the value shown by the bar.

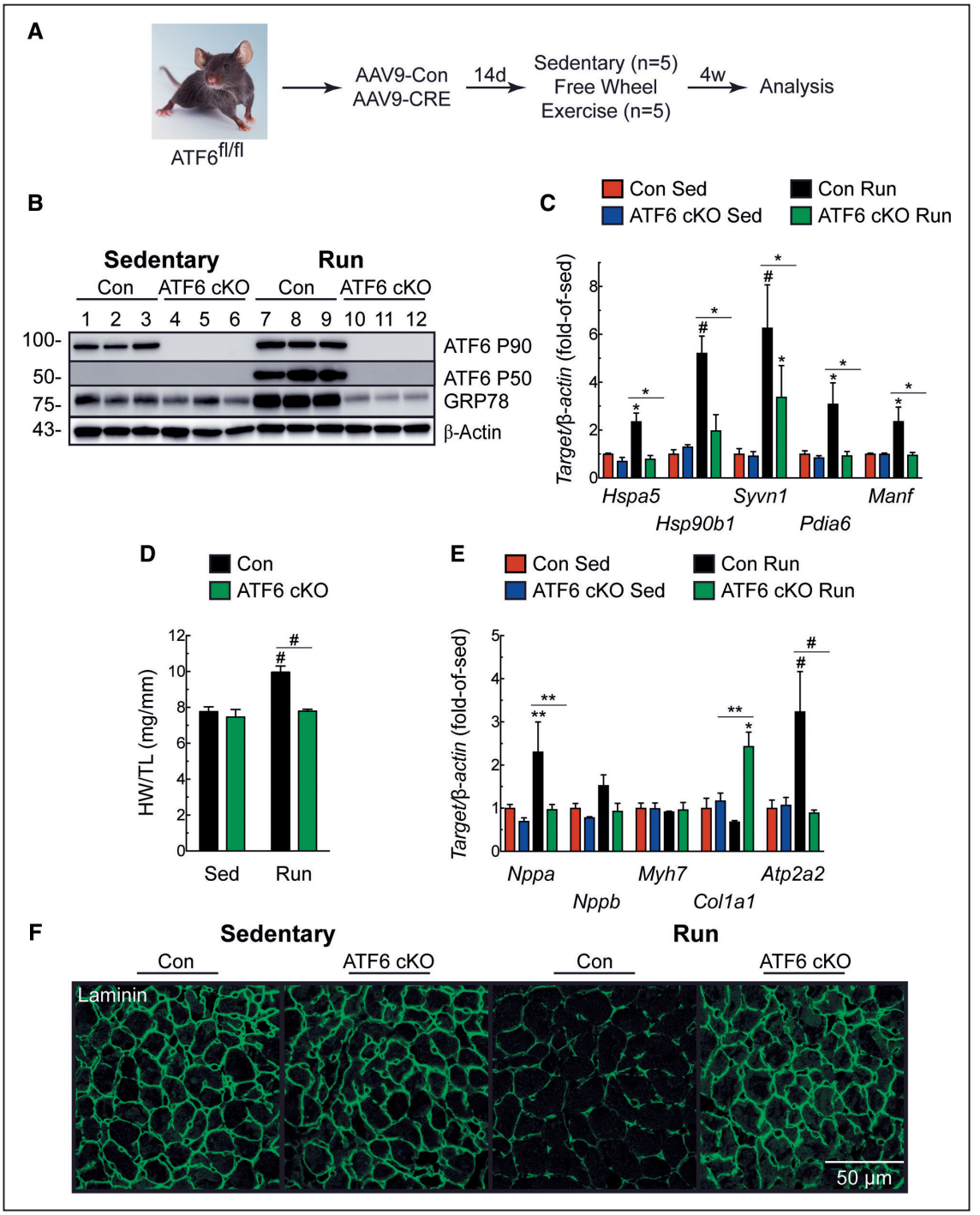

Figure 2. Effect of cardiac myocyte-specific *ATF6* (activating transcription factor 6α) gene deletion in hearts of mice subjected to free-wheel exercise. A, Protocol for adeno-associated virus (AAV) 9 administration to ATF6$^{fl/fl}$ mice and free-wheel exercise. **B**, Immunoblot of left ventricular extracts from Con or ATF6 cKO (conditional knockout) mice. **C**, mRNA levels for ATF6 target genes determined by quantitative real-time polymerase chain reaction (qRT-PCR). **D**, Heart weights/tibia lengths (HW/TL). **E**, mRNA levels for fetal genes determined by qRT-PCR. **F**, Immunocytofluorescence microscopy analysis of mouse heart sections for laminin (green). Data are mean±SEM. Echocardiography details are in Online Table II. **P*≤0.05, ***P*≤0.01, #*P*≤0.001.

the presence of a growth stimulus. Accordingly, we focused on *Rheb* as a candidate gene through which ATF6 might contribute to cardiac hypertrophy, pursuing the hypothesis that increased *Rheb* gene expression and subsequent mTORC1 activation under growth conditions are *Atf6* dependent. The upregulation of *RHEB* by ATF6 in mouse hearts observed by RNA sequencing was confirmed by quantitative real-time polymerase chain reaction (Online Figure IIB). Consistent with ATF6 as a possible transcriptional inducer of *Rheb* was our finding that the *Rheb* promoter has 2 potential ATF6-binding sites, which we call ER stress response elements (ERSEs)-1 and 2 (Figure 3B). Chromatin immunoprecipitation showed that ATF6 binds to

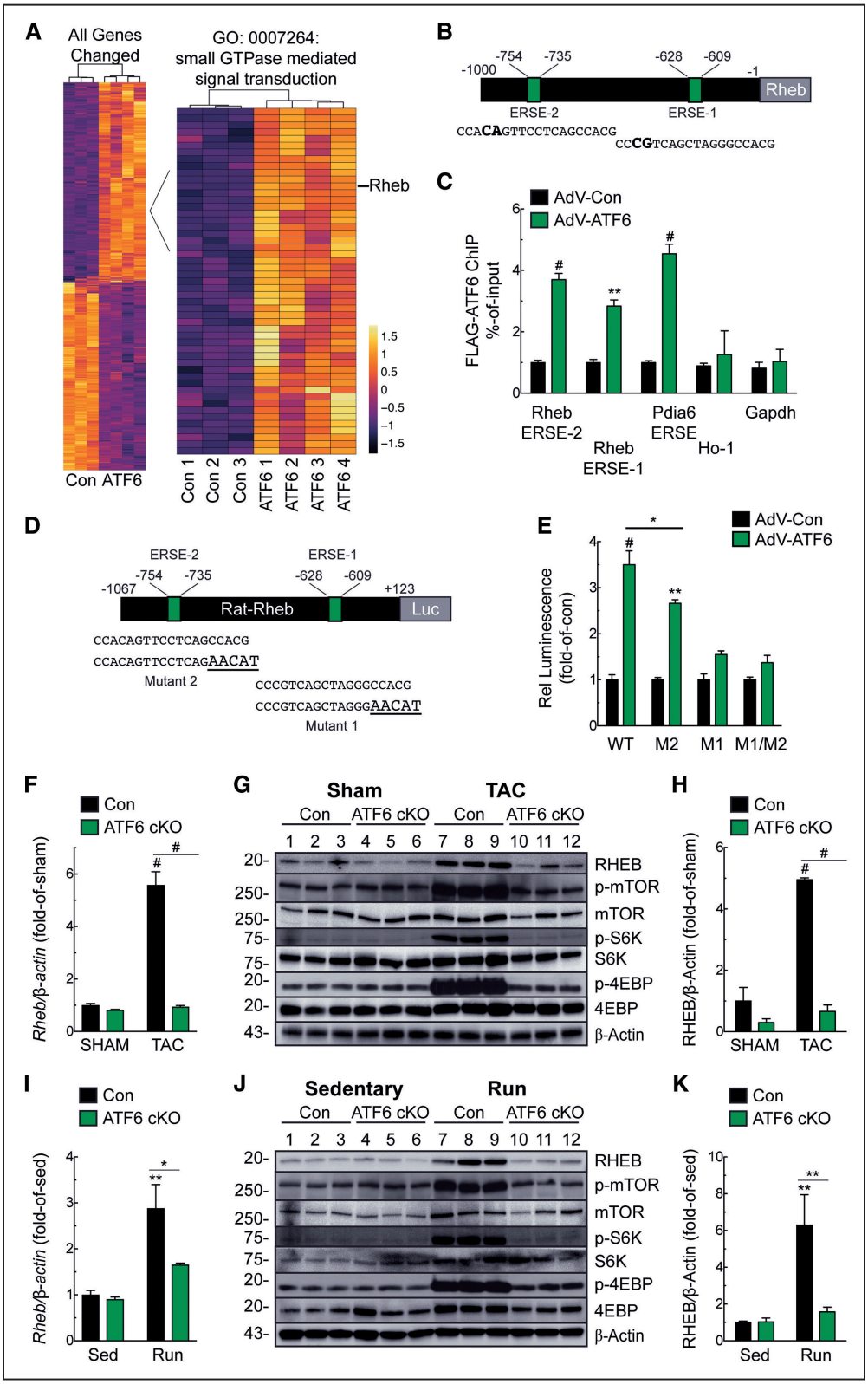

Figure 3. Regulation of Rheb (Ras homologue enriched in brain) expression by ATF6 (activating transcription factor 6α). A, Heat map of transcript profiling showing *Z* score-transformed reads per kilobase per million mapped read values with hierarchical clustering of transcripts of control and ATF6 transgenic mouse hearts. Differentially expressed genes with *P* values and FDR ≤0.05 and a subset of genes annotated with term GO:0007264 are shown. All the genes increased or decreased by ATF6 are in Online Table III. **B**, Locations of consensus ATF6-binding motifs, that is, endoplasmic reticulum stress response element (ERSE)-1 and 2 and their sequences in the *RHEB* gene 5′-flanking region. Nucleotide differences from canonical ERSE elements are bold. **C**, Neonatal rat ventricular myocytes (NRVMs) were infected with AdV encoding control or FLAG-ATF6 [1–373] (active form) and then ATF6 binding to endogenous ERSE-1 or ERSE-2, as well as to the endogenous *PDIA6* ERSE, used here as a positive control, and the negative control targets *ho-1* and *gapdh* were examined by chromatin immunoprecipitation (ChIP; n=3). (*Continued*)

Figure 3 Continued. **D**, Locations of ERSE-1 and 2 in the *RHEB* 5′-flanking region, their sequences (lower case), and the mutations that were made (bold and upper case). **E**, NRVMs were transfected with rat-*rheb*(-1067/+123)-Luc WT (wild type), M2, M1, or M1/M2 then infected with AdV FLAG-ATF6 (1–373). Then, 48 h later, luciferase activity was measured in extracts (n=6). **F–H**, mRNA for *RHEB* determined by quantitative real-time polymerase chain reaction (qRT-PCR; **F**) and Rheb protein and mTOR (mammalian/mechanistic target of rapamycin) pathway components measured by immunoblots (**G**) and quantified by densitometry (**H**) from Con or ATF6 cKO (conditional knockout) mouse heart extracts after 7 d of Sham or transverse aortic constriction (TAC). **I–K**, mRNA for *RHEB* determined by qRT-PCR (**I**) and Rheb protein and mTOR pathway component immunoblots (**J**) and quantified by densitometry (**K**) from Con or ATF6 cKO mouse heart extracts after 4 wk of sedentary or free-wheel exercise (Run). Data are mean±SEM. **P*≤0.05, ***P*≤0.01, #*P*≤0.001.

both sites in the *RHEB* gene in neonatal rat ventricular myocytes (NRVMs; Figure 3C). The progressive decline in *RHEB* promoter activity in plasmids that encode 5′-truncation deletions of the rat-*RHEB* promoter driving luciferase demonstrated the importance of these putative ERSEs in ATF6-mediated *RHEB* promoter activation (Online Figure IIC). To mechanistically investigate the functional involvement of these ERSEs further, we mutated either or both ERSEs (Figure 3D). Mutating either ERSE decreased ATF6 *RHEB* promoter activation by ATF6; however, the promoter-proximal site, that is, ERSE-1, appeared to have the largest effect (Figure 3E). To determine whether ATF6 is sufficient to induce *Rheb* in the heart, in vivo, mice were injected with a recombinant AAV9 that encodes activated ATF6 (ie, ATF6 [1–373]). Activated ATF6 increased *RHEB* mRNA and protein in the heart (Online Figure IID through IIF). These results are the first demonstration in any cell type that ATF6 induces *RHEB*, implicating ATF6 as a critical link between growth stimuli and mTORC1 activation.

RHEB Induction During Pressure Overload and Exercise Requires ATF6

We found that *RHEB* was strongly induced in Con mice after either TAC or exercise but not in ATF6 cKO mouse hearts (Figure 3F through 3K). Thus, ATF6 is necessary for the upregulation of RHEB in these models of cardiac hypertrophy, in vivo. Because RHEB is required for mTORC1 activation in response to a growth stimulus, we assessed mTORC1 pathway activation. As expected, pressure overload and exercise both activated mTORC1, as shown by increased phosphorylation of mTORC1 (Ser2448), S6K (p70 ribosomal S6 kinase; Thr389), and eukaryotic translation initiation factor 4E-BP1 (4E-binding protein 1; Thr37/46); however, mTORC1 activation was blunted in ATF6 cKO mouse hearts (Figure 3G and 3J), consistent with the key role for ATF6 in mTORC1 activation by growth stimuli. To examine whether ATF6 might affect other signaling pathways leading to mTORC1 activation, we assessed the phosphorylation of Akt on Ser308 and the phosphorylation of TSC2, both of which lie upstream of Rheb in the mTORC1-signaling pathway. We found that pressure overload increased phosphorylation of Akt (Thr308) and TSC2 (Thr1462), as expected; however, in contrast to Rheb expression, neither of these phosphorylation events were affected by *ATF6* deletion (Online Figure IIIA). Thus, the deficit in mTORC1 activation in ATF6 cKO mice must reside downstream of Akt and TSC2 (ie, Rheb). We also examined whether ATF6 deletion affected other well-known canonical hypertrophy signaling pathways but found that neither phosphorylation of Akt on Ser-473, Erk phosphorylation (Online Figure IIIA), or calcineurin activation (Online Figure IIIB) were affected by ATF6 deletion. These results pinpoint the growth deficit in the ATF6 cKO mouse hearts to the inability to upregulate Rheb.

RHEB Is Required for Phenylephrine and IGF1-Induced Cardiac Myocyte Growth

To explore the mechanistic relationship between *ATF6* and *RHEB*, we used *RHEB* and *ATF6* loss-of-function approaches in NRVM treated with the α_1-adrenergic receptor agonist, phenylephrine, or IGF1 (insulin-like growth factor 1), which recapitulate much of the intracellular signaling during pressure overload or exercise-induced hypertrophy, respectively.[29] Knocking down either *ATF6* or *RHEB* abrogated the effects of phenylephrine or IGF1 on cardiac myocyte hypertrophy, fetal gene induction, ATF6 target gene induction, and mTORC1 signaling (Figures 4A through 4E and 5A through 5E; Online Figure IVA through IVC) but had no effect on mTORC2 signaling, as assessed by phosphorylation of Akt on Ser-473 (Online Figure IVD and IVE). To further substantiate the results with *Rheb* siRNA, we used a different Rheb loss-of-function approach involving the Rheb inhibitor, lonafarnib.[30] Lonafarnib mimicked the effects of *Rheb* siRNA on phenylephrine and IGF1-mediated ATF6 activation, mTORC1 signaling, *ATF6* gene induction, and growth in NRVM (Online Figure V).

To complement *ATF6* loss-of-function approach, we used a gain-of-function approach, examining the effects of ectopic expression of *ATF6* and *RHEB*. In the absence of a growth stimulus, ectopic expression of *ATF6* did not increase myocyte growth, as expected, because of the absence of mTORC1 activation under these conditions (Online Figure VIA; Con). Either phenylephrine or IGF1 increased myocyte growth, which was completely blocked by the mTORC1 inhibitor, rapamycin, as expected (Online Figure VIA; phenylephrine and IGF1, red versus blue). Ectopic ATF6 augmented the growth-promoting effects of phenylephrine and IGF1, which were also completely blocked by rapamycin (Online Figure VIA; phenylephrine and IGF1, black and green). Moreover, ectopic ATF6 slightly augmented phenylephrine and IGF1-stimulated NRVM growth; however, it was not able to restore growth in cells treated with either *RHEB* siRNA or lonafarnib (Online Figure VIB and VIC). As expected, ectopic expression of *RHEB* had no effect in the absence of a growth stimulus; however, on a growth stimulus, the loss of growth and mTORC1 activation seen with *ATF6* siRNA were completely restored by ectopically expressed *RHEB* (Figures 4F through 4H and 5F through 5H).

Mechanistic Relationship Between Growth Signaling and the Unfolded Protein Response

The UPR (unfolded protein response), which in addition to ATF6, is mediated by PERK (eukaryotic translation initiation factor 2-alpha kinase 3) and IRE1 (serine/threonine-protein kinase/endoribonuclease),[5] is activated by the misfolding of proteins induced by a variety of chemical and pathophysiological treatments, most of which do not promote growth. In fact, the UPR is not widely considered to be growth promoting. Accordingly, because we found here that ATF6 can be activated during growth,

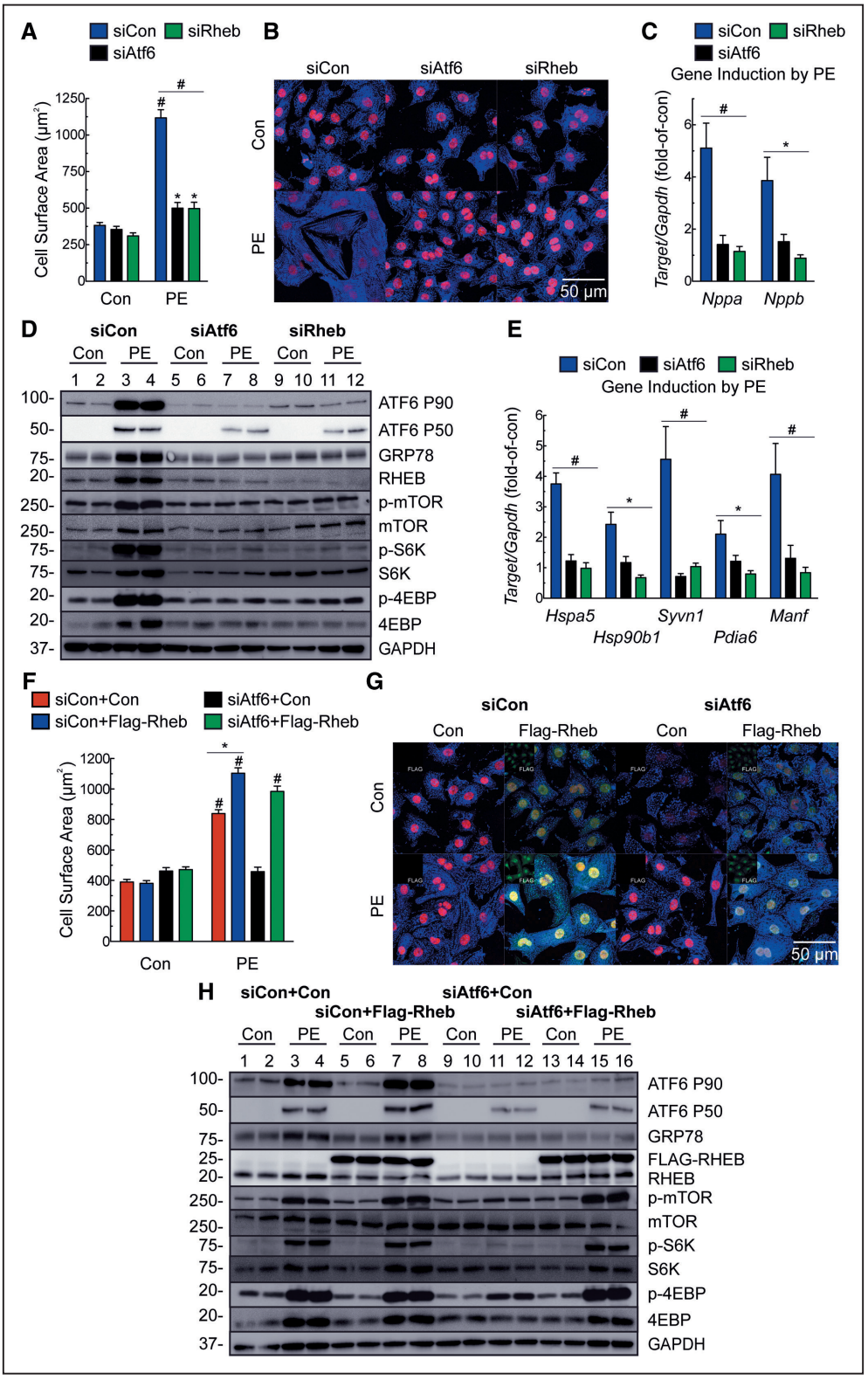

Figure 4. Effects of *ATF6* (activating transcription factor 6α) and *RHEB* (Ras homologue enriched in brain) knockdown, and ectopic Rheb expression on phenylephrine-induced hypertrophy in cultured cardiac myocytes. A–E, Neonatal rat ventricular myocytes (NRVMs) were transfected with a nontargeted siRNA (siCon) or with siRNAs targeted to either rat *ATF6* (siAtf6) or *RHEB* (siRheb), and then treated±phenylephrine (PE; 50 μM) for 48 h. **A**, Cell surface area was determined by photomicroscopy and morphometry (n=6). **B**, Immunocytofluorescence microscopy (ICF) of NRVM for α-actinin (blue) and TOPRO-3 (red; bar=50 μm). **C**, Quantitative real-time polymerase chain reaction (qRT-PCR) examination of *Nppa* and *Nppb*. Values are expressed as fold-of-control cardiac myocytes in the absence of PE (n=6). **D**, Immunoblot of NRVM. **E**, mRNA for ATF6 target genes determined by qRT-PCR. Values are expressed as fold-of-control myocytes in the absence of PE (n=3). **F–H**, NRVMs were transfected with a control plasmid or a plasmid encoding Flag-Rheb and either siCon or siAtf6, followed by treatment±PE for 48 h. Cell surface area (**F**) was determined by morphometry after ICF (**G**). NRVMs were stained for FLAG (green; isolated channel displayed in inset), α-actinin (blue), and TOPRO-3 (red; bar=50 μm). Only FLAG-positive cells were used for cell surface area analysis (n=3). **H**, Immunoblot of NRVM. Data are mean±SEM. *P≤0.05, **P≤0.01, #P≤0.001.

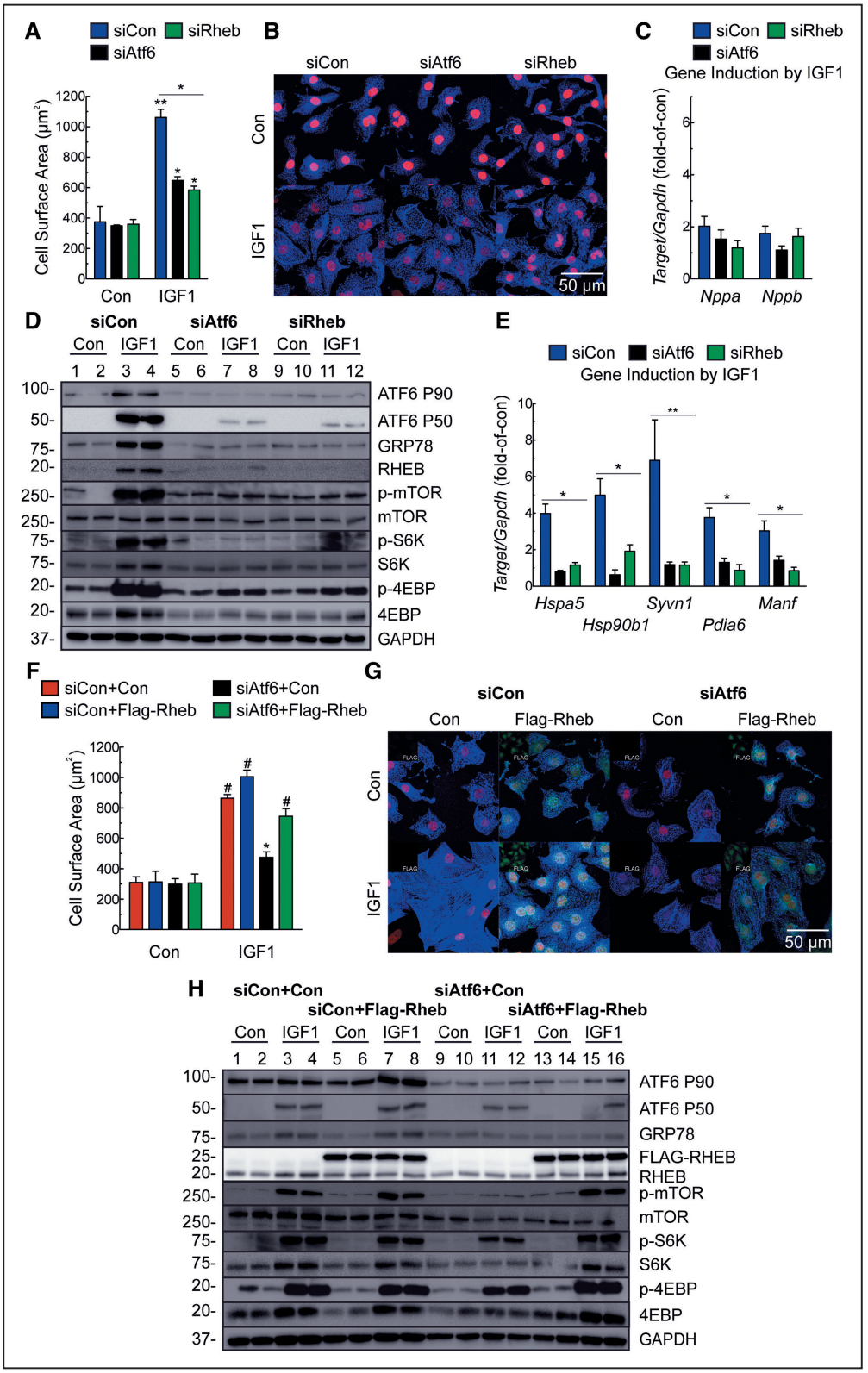

Figure 5. Effects of *ATF6* (activating transcription factor 6α) and *RHEB* (Ras homologue enriched in brain) knockdown and ectopic Rheb expression on insulin-like growth factor 1–induced hypertrophy in cultured cardiac myocytes. A–E, Neonatal rat ventricular myocytes (NRVMs) were transfected with siCon, siAtf6 or siRheb and then treated±IGF1 (insulin-like growth factor 1; 100 ng/mL) for 48 h. **A**, Cell surface area was determined by morphometry after immunocytofluorescence microscopy (ICF; n=6). **B**, ICF of NRVM for α-actinin (blue) and TOPRO-3 (red; bar=50 μm). **C**, Quantitative real-time polymerase chain reaction (qRT-PCR) for *Nppa* and *Nppb*. Values are fold-of-control myocytes in the absence of IGF1 (n=6). **D**, Immunoblot of NRVM. **E**, mRNA levels of ATF6 target genes determined by qRT-PCR. Values are fold-of-control myocytes in the absence of IGF1 (n=3). **F–H**, NRVMs were transfected with a control plasmid or a plasmid encoding Flag-Rheb and then either siCon or siAtf6, followed by treatment±IGF1 for 48 h. Cell surface area (**F**) was determined by morphometry after ICF (**G**). NRVMs were stained for FLAG (green; isolated channel displayed in inset), α-actinin (blue), and TOPRO-3 (red; bar=50 μm). Only FLAG-positive cells were used for cell surface area analysis (n=3). **H**, Immunoblot of NRVM. Data are mean±SEM. **P*≤0.05, ***P*≤0.01, #*P*≤0.001.

we assessed how growth affected the other arms of the UPR. We found that phenylephrine and IGF1 activated all 3 arms of the UPR in a rapamycin-sensitive manner (Online Figure VIIA), indicating that mTORC1 activation is required for UPR activation during growth. We then individually knocked down *ATF6*, *PERK*, and *IRE1* and found that only ATF6 knockdown blunted growth (Online Figure VIIB and VIIC). To ensure that the effects of ATF6 on growth are dependent on the transcriptional effects of ATF6, we showed that NRVM infected with adenovirus-ATF6 [1–373] (active) exhibited increased growth in response to phenylephrine, especially when endogenous ATF6 was knocked down; however, adenovirus-ATF6 [94–373] (trancriptionally inactive) did not (Online Figure VIID).

Next, we examined the effect on mTORC1 signaling of other UPR stimulators that do not affect growth, such as tunicamycin, which increases ER protein misfolding by inhibiting protein glycosylation in the ER. In contrast to phenylephrine, activation of ATF6 by tunicamycin was not dependent on *RHEB* (Figure 6A and 6B). Additionally, although *RHEB* knockdown blocked phenylephrine and IGF1-mediated induction of ATF6 target genes (Figures 4E and 5E), it had no effect on tunicamycin-mediated induction of ATF6 target genes (Figure 6C). Thus, there are RHEB/growth-dependent and RHEB/growth-independent pathways that lead to ATF6 activation and induction of ATF6 target genes.

Stimulus-Dependent Differential Induction of ATF6 Target Genes

We dived deeper into the mechanism of RHEB/growth-dependent and RHEB/growth-independent pathways of ATF6 activation. We previously showed that ATF6 induces some proteins targeted to the ER, where they enhance protein folding (eg, *HSPA5*/*GRP78*), and others located outside the ER, where they serve other functions. One example of the latter is our finding that ischemia/reperfusion activates ATF6-dependent induction of *CAT*, which resides in peroxisomes and neutralizes damaging ROS (reactive oxygen species). Here, we provide an additional example of an ATF6-inducible gene, *RHEB*, that encodes a protein that resides outside the ER. Because of the differences in the locations and functions of Hspa5, CAT, and Rheb, we posited that they might be differentially induced by treatments that cause ER protein misfolding, ie, tunicamycin or oxidative stress, ie, ischemia/reperfusion, but do not induce growth, or to a treatment that induces growth, ie, phenylephrine. Although, for the most part, all 3 genes were induced by all of the treatments, the quantitative nature of induction differed depending on the treatments, such that tunicamycin, simulated ischemia/reperfusion (sI/R), and phenylephrine had the greatest effects on induction of *Hspa5*, *Cat*, and *Rheb*, respectively (Figure 6D). Notably, *Cat* induction was highly selective, showing an ≈6-fold induction by sI/R and much less induction by either tunicamycin or phenylephrine (Figure 6D; *Cat*). Remarkably, *RHEB* induction was also highly selective, showing the least induction by tunicamycin or sI/R, while being induced by >5-fold by phenylephrine (Figure 6D; *Rheb*). Importantly, all of these effects depended on ATF6 (Figure 6E).

To dissect this stimulus-dependent differential gene induction further, we showed that promoter/luciferase reporter constructs for *Hspa5*, *Cat*, and *Rheb* (Figure 6F) were also differentially induced by tunicamycin, sI/R, and phenylephrine, mimicking mRNA induction (Figure 6G). Importantly, as with the mRNA, all of these effects required ATF6 (Figure 6H).

We hypothesized that these stimulus-specific effects of ATF6 on *Hspa5*, *Cat*, and *Rheb* could be the result of the stimulus-dependent binding of ATF6 to the ERSEs in these genes. To test this hypothesis, we developed a new method for measuring ATF6 binding to the *HSPA5*, *CAT*, and *RHEB* promoters in cells treated with tunicamycin, sI/R, or phenylephrine. To this end, we generated a recombinant adenovirus FLAG full-length p90 ATF6, that is, ATF6 (1–670), which remains in the ER in the absence of ER stress and, therefore, cannot bind to ERSEs. NRVM expressing p90 ATF6 were treated with tunicamycin, sI/R, or phenylephrine, each of which induce the formation of the N-terminal, active p50 form of ATF6, so it can bind to ERSEs. Chromatin immunoprecipitation demonstrated that the binding of ATF6 to these genes differed, depending on the stimulus, mimicking the mRNA induction and promoter activation (Figure 6I). These effects were not seen with adenovirus encoding only FLAG, verifying ATF6 specificity (Figure 6J). This shows, for the first time in any cell type, that ATF6 can be activated by a broad spectrum of conditions that affect proteostasis in a variety of ways, yet the relative induction of ATF6 targets differs in a condition-dependent manner.

Ectopic Expression of RHEB Restores Cardiac Growth to ATF6 cKO Mouse Hearts

Next, we assessed the effects of ectopic expression of *RHEB* in the heart, in vivo, using a new recombinant AAV9-RHEB (Figure 7A). In ATF6 cKO mice, AAV9-RHEB effectively restored the loss of mTORC1 signaling, hypertrophic growth, and cardiac function, as well as the hypertrophic and *ATF6* gene programs in response to TAC (Figure 7B through 7F; Online Table IV). Thus, it is by increasing RHEB that ATF6 influences mTORC1 signaling and subsequent cardiac myocyte growth, fetal gene expression, and ATF6 target gene expression.

ATF6 Activation in Response to Growth Requires mTORC1 Activation, Protein Synthesis, and Protein Misfolding

To this point, we had shown that mTORC1 and ATF6 activation were dependent on each other under the growth conditions examined. To account for this interdependence, we posited a temporal sequence of events, wherein the initial event after a growth stimulus is mTORC1 activation, which depends on basal levels of Rheb (Figure 8A, step 1). This initial mTORC1 activation precedes but drives initial increases in protein synthesis that places demands on the protein-folding machinery (Figure 8A, step 2), which activates ATF6. Then, ATF6 serves canonical and noncanonical roles (Figure 8A, steps 3 and 4), the latter of which includes *RHEB* induction (Figure 8A, step 5), which is necessary to sustain mTORC1 activation (Figure 8A, step 6) and the subsequent continued increases in protein synthesis that are required for growth and cardiac myocyte hypertrophy (Figure 8A, step 7). To examine this hypothesis, a TAC time course was performed. At 3 hours of TAC—a time when mTORC1 is activated but protein synthesis has not yet increased—mTORC1 signaling was activated, but ATF6 was not activated and *RHEB* was not induced (Figure 8B, 3 hours). However, at both 2 and 7 days of TAC,

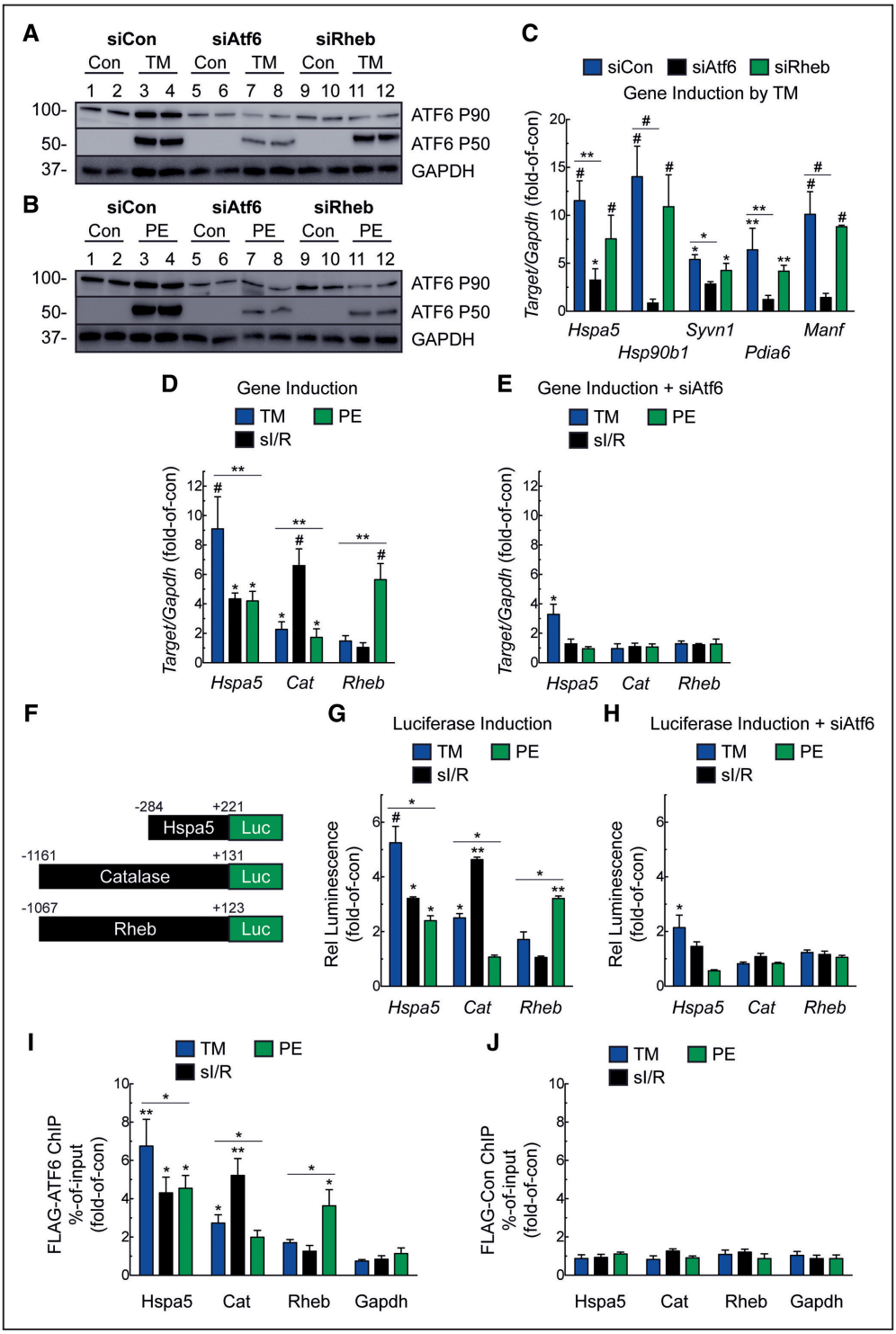

Figure 6. Examination of Rheb (Ras homologue enriched in brain) requirement for growth-dependent but not growth-independent activation of the ATF6 (activating transcription factor 6α). **A** and **B**, Neonatal rat ventricular myocytes (NRVMs) were transfected with siCon, siAtf6, or siRheb and then treated±tunicamycin (TM; 10 μg/mL; **A**) or PE (50 μM; **B**) for 24 h and then analyzed for ATF6 activation by immunoblotting. **C**, mRNA levels for ATF6 target genes determined by quantitative real-time polymerase chain reaction (qRT-PCR). Values are fold-of-control, that is, not treated with TM (n=6). **D** and **E**, NRVMs were transfected with siCon (**D**) or siAtf6 (**E**) and then treated±TM (10 μg/mL) or PE (50 μM) for 24 h, or subjected to simulated ischemia/reperfusion (sI/R; 8 h of sI, followed by 24 h of reperfusion) and mRNA for ATF6 target genes determined by qRT-PCR (n=6). **F**, Diagram of constructs that encode luciferase driven by the *grp78*, catalase, and *rheb* 5′-flanking region. **G** and **H**, NRVMs were transfected with human-*grp78*(−284/+221)-Luc WT, rat-catalase(−1161/+131)-Luc WT, or rat-*rheb*(−1067/+123)-Luc WT and then transfected with siCon (**G**) or siAtf6 (**H**), then treated±TM (10 μg/mL) or PE (50 μM) for 24 h, or subjected to sI/R and luciferase activity measured in extracts (n=6). **I** and **J**, NRVM infected with AdV FLAG-ATF6 [1–670] (**I**) or control (**J**), and then ATF6 binding to the endogenous *grp78*, catalase, or *rheb* genes, as well as to the negative control gene, *gapdh*, examined by ChIP under the same experimental conditions described above (n=3). Data are mean±SEM. **P*≤0.05, ***P*≤0.01, #*P*≤0.001.

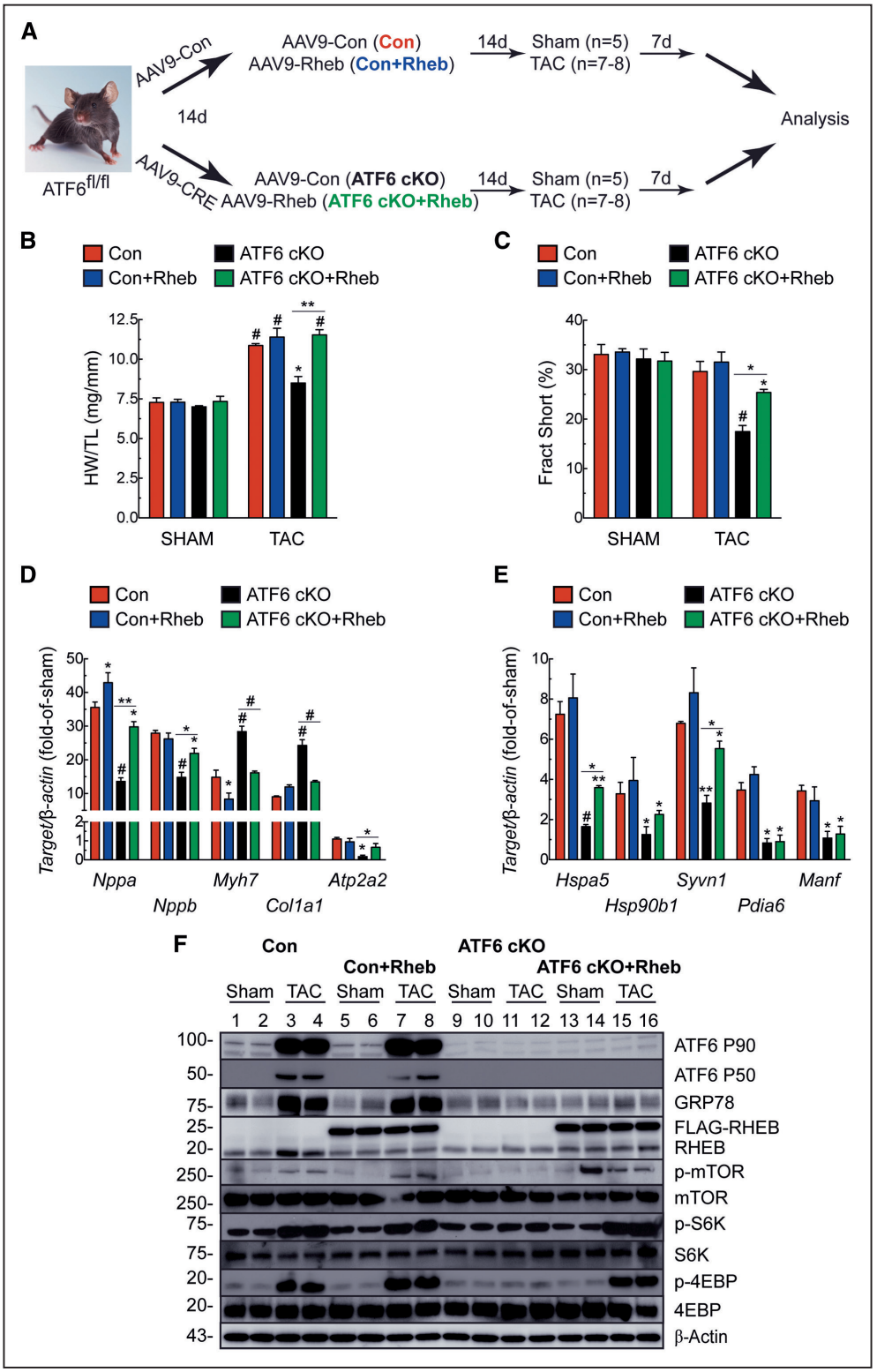

Figure 7. Effect of cardiac myocyte-specific ectopic Rheb (Ras homologue enriched in brain) expression in *ATF6* (activating transcription factor 6α) gene deleted mouse hearts subjected to transverse aortic constriction (TAC). A, Experimental protocol for adeno-associated virus (AAV) 9 administration to ATF6$^{fl/fl}$ mice and TAC. **B**, Heart weights/tibia lengths (HW/TL). **C**, Fractional shortening (%), as determined by echocardiography (Online Table IV). **D**, mRNA for fetal genes determined by qRT-PCR. **E**, mRNA for ATF6 target genes determined by qRT-PCR. **F**, Immunoblots of left ventricular extracts. Data are mean±SEM. *P≤0.05, **P≤0.01, #P≤0.001.

when protein synthesis is increased, mTORC1 signaling and ATF6 were activated, and *RHEB* was induced (Figure 8B, 2 and 7 days). As expected, heart weights increased as a function of TAC time from 3 hours to 7 days (Figure 8C; Online Table V). Thus, mTORC1 activation occurred soon after TAC and preceded ATF6 activation. Further supporting our hypothesis

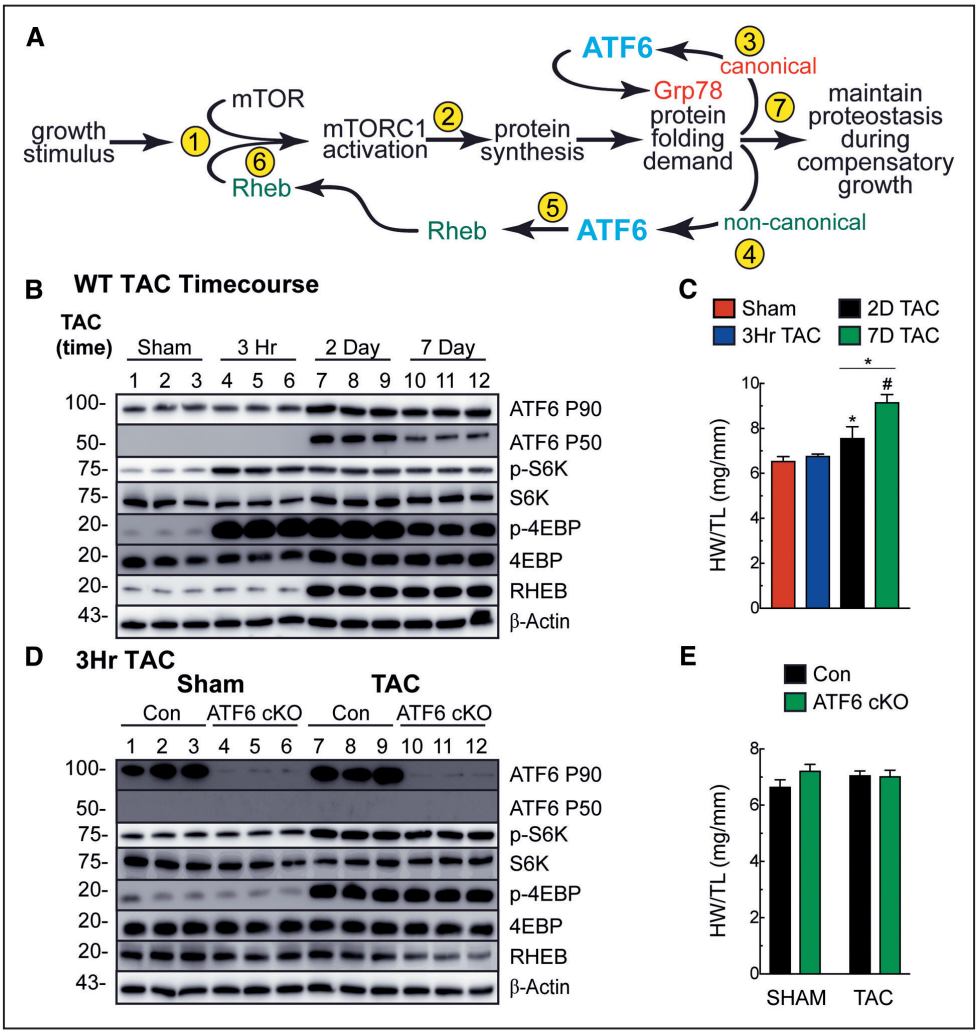

Figure 8. Mechanism whereby ATF6 (activating transcription factor 6α) acts as a nodal regulator of both protein synthesis and protein folding during cardiac hypertrophy. A, Shown are the temporal sequence of steps involved in mediating the initial (steps 1–4) and sustained (steps 5–7) aspects of growth and the interdependent roles of mTORC1 (mammalian/mechanistic target of rapamycin complex 1) and ATF6. **B** and **C**, Immunoblot of left ventricular (LV) extracts (**B**) heart weight/tibia length (HW/TL; **C**) from WT mice subjected to transverse aortic constriction (TAC) for 3 h, 2 d, or 7 d. Echocardiography details are provided in Online Table V. **D** and **E**, Immunoblot of LV extracts (**D**) and heart weights/tibia lengths (HW/TL; **E**) from Con or ATF6 cKO (conditional knockout) mice subjected to 3 h of TAC. Echocardiography details are provided in Online Table VI. Data are mean±SEM. **P*≤0.05, #*P*≤0.001.

that initially mTORC1 activation precedes ATF6 activation were results of a 3-hour TAC experiment in ATF6 cKO mice, where, in contrast to longer times of TAC (ie, 7 days; Figure 3G), the deletion of ATF6 did not affect mTORC1 activation (Figure 8D). As expected, heart weights did not change under these conditions (Figure 8E; Online Table VI).

Consistent with these results, when examining the effect of phenylephrine and IGF1 at the earliest time points, just prior to the time when protein synthesis is the greatest in NRVM, knocking down *ATF6* did not affect mTORC1 activation (Online Figure VIIIA), but again, ATF6 activation was rapamycin dependent (Online Figure VIIIB). Moreover, inhibiting protein synthesis with cycloheximide had no effect on mTORC1 activation at these short times of phenylephrine or IGF1 treatment, but impaired ATF6 activation and *RHEB* induction, indicating that protein synthesis is required for ATF6 activation and subsequent *RHEB* induction (Online Figure VIIIC). Finally, in NRVM treated with the chemical chaperone, 4PBA, phenylephrine, and IGF1 activated mTORC1; however, ATF6 was not activated, and *RHEB* was not induced (Online Figure VIIID), indicating the increase in protein-folding demand driven by increases in protein synthesis is responsible for activating ATF6.

Discussion

ATF6 Is Required for Growth of the Heart

Although previous studies reported increased expression of a few ER stress genes in mouse models of pressure overload, implicating ER protein misfolding,[31–34] before this study neither the activation nor the roles for ATF6 in cardiac myocytes during cardiac growth had been examined. Here, we showed for the first time that ATF6, a major mediator of the UPR, is activated by diverse growth stimuli and that ATF6 is required for growth of the heart in response to these stimuli. We determined that the mechanism of this effect involves ATF6-mediated induction of *RHEB* (Figure 8A). It was surprising to find that ATF6 is required for heart growth, considering the UPR is not widely known to be involved in growth processes. However, this noncanonical role for

ATF6 complements its canonical role as a sensor of misfolded proteins in the ER and, as such, a sensor of increases in protein-folding demand, which occur during growth. Thus, ATF6 maintains proteostasis and proteome integrity when the heart is stimulated to grow in a compensatory manner.

ATF6 Exhibits Stress-Specific Transcriptional Gene Induction

We also found that, depending on the stimulus, ATF6 target genes are differentially expressed because of the unique effects that the stresses have on ATF6 binding to, and thus, transcriptional activation of ATF6 target genes. Such differential ATF6 target gene induction by treatments that all activate ATF6 suggests that there are yet-to-be-described regulatory layers that fine-tune the *ATF6* gene program to best adapt to the conditions. Some possible mechanisms that could contribute to this differential expression are beginning to emerge, as it has been shown that ATF6 can interact with other transcription factors, such as Nrf1 (nuclear respiratory factor 1), PGC1α and β (peroxisome proliferator-activated receptor gamma coactivator 1-alpha and -beta), and ERRγ (estrogen-related receptor gamma),[35–37] which changes the transcriptional programming in ways that fine-tune ATF6 target gene induction. Additionally, it was recently shown that ATF6 can be differentially activated by lipids and proteotoxic stress at least partly by virtue of separate activation domains on ATF6 for these 2 different stresses.[38]

Rheb in the Heart

Rheb was originally documented as an mTORC1 activator in the brain[39]; this role has been demonstrated in numerous other tissues and organs.[17,40,41] Global deletion of *Rheb* is embryonic lethal, in part, because of cardiac defects,[42] demonstrating the importance of Rheb-mediated mTORC1 activation in heart growth and development. The growth-promoting effect of *Rheb* gain-of-function was demonstrated in adult rat ventricular myocytes transfected with adenovirus encoding *Rheb*.[43] However, overexpression of *Rheb* in transgenic mice increased infarct size, in part, because Rheb inappropriately decreased autophagy, which is adaptive in this disease setting.[44] Pharmacological inhibition of Rheb in mice subjected to TAC for 3 weeks was cardioprotective.[14] These findings differ from our study, perhaps because different times after TAC were studied or different approaches were used to decrease Rheb. It is also possible that Rheb induction and mTORC1 activation have different roles in a severe afterload-induced hypertrophy model, such that acute activation works in a compensatory manner, but chronic activation drives decompensation. The αMHC-CRE–dependent conditional deletion of *Rheb* from mouse cardiac myocytes resulted in atrophic hearts, heart failure, and death within 1 to 2 weeks after birth—a time frame that aligns with the time of αMHC expression after birth.[12,45] Although there have been no studies before ours mechanistically connecting *Atf6* with *Rheb* induction, one study in tumor cells[46] and another in the setting of Huntington disease[47] have implicated such a connection and therefore support the findings reported here.

Feedback Regulation of ATF6-Mediated Growth

Our study describes a mechanism whereby ATF6 matches protein synthesis with folding in times of increased growth; because this constitutes a positive feedback mechanism, we reason that there must also be mechanisms that interrupt the positive nature of the feedback, thereby limiting the rate of growth driven by the ATF6-Rheb-mTORC1 axis. One such mechanism might involve Rheb itself, which has been shown to activate PERK.[48] Mechanisms such as this underscore the complexities of proteostasis, raising questions about how Rheb switches from protein synthesis activator to inhibitor.

Conclusions

The results of our study firmly place ATF6 in a critical position as a determinant of cardiac growth (Figure 8A). Moreover, because ATF6 is ubiquitously expressed, our findings underscore the widespread importance of the ATF6-Rheb-mTORC1 growth signaling axis described here in noncardiac cells and tissues in addition to the heart.

Acknowledgments

We thank Dr Gokhan S. Hotamisligil (Harvard T.H. Chan School of Public Health, Boston, MA) for the ATF6α$^{fl/fl}$ mice.

Sources of Funding

E.A. Blackwood was supported by the American Heart Association (17PRE33670796), the National Institutes of Health (1F31HL140850), the Rees-Stealy Research Foundation and San Diego State University (SDSU) Heart Institute, the Inamori Foundation, and the ARCS Foundation, Inc, San Diego Chapter. C. Hofmann was supported by Boehringer Ingelheim Fonds Travel Grant, the DZHK (German Centre for Cardiovascular Research) Mobilitätsprogramm, and the Deutsche Herzstiftung. O.J. Müller was supported by the DZHK and by the BMBF (German Ministry of Education and Research). S. Doroudgar was supported by an Excellence Grant from the DZHK and Department of Cardiology, Angiology, and Pneumology, University Hospital Heidelberg. C.C. Glembotski was supported by (National Institutes of Health) grants R01 HL75573, R01 HL104535, and P01 HL085577.

Disclosures

None.

References

1. Balch WE, Morimoto RI, Dillin A, Kelly JW. Adapting proteostasis for disease intervention. *Science*. 2008;319:916–919. doi: 10.1126/science.1141448
2. Glembotski CC. Roles for the sarco-/endoplasmic reticulum in cardiac myocyte contraction, protein synthesis, and protein quality control. *Physiology (Bethesda)*. 2012;27:343–350. doi: 10.1152/physiol.00034.2012
3. Gidalevitz T, Stevens F, Argon Y. Orchestration of secretory protein folding by ER chaperones. *Biochim Biophys Acta*. 2013;1833:2410–2424. doi: 10.1016/j.bbamcr.2013.03.007
4. Glembotski CC. Roles for ATF6 and the sarco/endoplasmic reticulum protein quality control system in the heart. *J Mol Cell Cardiol*. 2014;71:11–15. doi: 10.1016/j.yjmcc.2013.09.018
5. Arrieta A, Blackwood EA, Glembotski CC. ER protein quality control and the unfolded protein response in the heart. *Curr Top Microbiol Immunol*. 2018;414:193–213. doi: 10.1007/82_2017_54
6. Zhu C, Johansen FE, Prywes R. Interaction of ATF6 and serum response factor. *Mol Cell Biol*. 1997;17:4957–4966.
7. Haze K, Yoshida H, Yanagi H, Yura T, Mori K. Mammalian transcription factor ATF6 is synthesized as a transmembrane protein and activated by proteolysis in response to endoplasmic reticulum stress. *Mol Biol Cell*. 1999;10:3787–3799. doi: 10.1091/mbc.10.11.3787
8. Luckey SW, Walker LA, Smyth T, Mansoori J, Messmer-Kratzsch A, Rosenzweig A, Olson EN, Leinwand LA. The role of Akt/GSK-3beta signaling in familial hypertrophic cardiomyopathy. *J Mol Cell Cardiol*. 2009;46:739–747. doi: 10.1016/j.yjmcc.2009.02.010
9. Bernardo BC, McMullen JR. Molecular aspects of exercise-induced cardiac remodeling. *Cardiol Clin*. 2016;34:515–530. doi: 10.1016/j.ccl.2016.06.002

10. Zhang D, Contu R, Latronico MV, et al. MTORC1 regulates cardiac function and myocyte survival through 4E-BP1 inhibition in mice. *J Clin Invest*. 2010;120:2805–2816. doi: 10.1172/JCI43008
11. Shende P, Plaisance I, Morandi C, Pellieux C, Berthonneche C, Zorzato F, Krishnan J, Lerch R, Hall MN, Rüegg MA, Pedrazzini T, Brink M. Cardiac raptor ablation impairs adaptive hypertrophy, alters metabolic gene expression, and causes heart failure in mice. *Circulation*. 2011;123:1073–1082. doi: 10.1161/CIRCULATIONAHA.110.977066
12. Tamai T, Yamaguchi O, Hikoso S, et al. Rheb (Ras homologue enriched in brain)-dependent mammalian target of rapamycin complex 1 (mTORC1) activation becomes indispensable for cardiac hypertrophic growth after early postnatal period. *J Biol Chem*. 2013;288:10176–10187. doi: 10.1074/jbc.M112.423640
13. Völkers M, Toko H, Doroudgar S, Din S, Quijada P, Joyo AY, Ornelas L, Joyo E, Thuerauf DJ, Konstandin MH, Gude N, Glembotski CC, Sussman MA. Pathological hypertrophy amelioration by PRAS40-mediated inhibition of mTORC1. *Proc Natl Acad Sci USA*. 2013;110:12661–12666. doi: 10.1073/pnas.1301455110
14. Wu X, Cao Y, Nie J, Liu H, Lu S, Hu X, Zhu J, Zhao X, Chen J, Chen X, Yang Z, Li X. Genetic and pharmacological inhibition of Rheb1-mTORC1 signaling exerts cardioprotection against adverse cardiac remodeling in mice. *Am J Pathol*. 2013;182:2005–2014. doi: 10.1016/j.ajpath.2013.02.012
15. Sciarretta S, Forte M, Frati G, Sadoshima J. New insights into the role of mTOR signaling in the cardiovascular system. *Circ Res*. 2018;122:489–505. doi: 10.1161/CIRCRESAHA.117.311147
16. Sancak Y, Peterson TR, Shaul YD, Lindquist RA, Thoreen CC, Bar-Peled L, Sabatini DM. The Rag GTPases bind raptor and mediate amino acid signaling to mTORC1. *Science*. 2008;320:1496–1501. doi: 10.1126/science.1157535
17. Durán RV, Hall MN. Regulation of TOR by small GTPases. *EMBO Rep*. 2012;13:121–128. doi: 10.1038/embor.2011.257
18. Betz C, Hall MN. Where is mTOR and what is it doing there? *J Cell Biol*. 2013;203:563–574. doi: 10.1083/jcb.201306041
19. Tee AR, Manning BD, Roux PP, Cantley LC, Blenis J. Tuberous sclerosis complex gene products, Tuberin and Hamartin, control mTOR signaling by acting as a GTPase-activating protein complex toward Rheb. *Curr Biol*. 2003;13:1259–1268.
20. Engin F, Yermalovich A, Nguyen T, Ngyuen T, Hummasti S, Fu W, Eizirik DL, Mathis D, Hotamisligil GS. Restoration of the unfolded protein response in pancreatic β cells protects mice against type 1 diabetes. *Sci Transl Med*. 2013;5:211ra156. doi: 10.1126/scitranslmed.3006534
21. Wang Y, Zhang Y, Ding G, May HI, Xu J, Gillette TG, Wang H, Wang ZV. Temporal dynamics of cardiac hypertrophic growth in response to pressure overload. *Am J Physiol Heart Circ Physiol*. 2017;313:H1119–H1129. doi: 10.1152/ajpheart.00284.2017
22. Nakamura A, Rokosh DG, Paccanaro M, Yee RR, Simpson PC, Grossman W, Foster E. LV systolic performance improves with development of hypertrophy after transverse aortic constriction in mice. *Am J Physiol Heart Circ Physiol*. 2001;281:H1104–H1112. doi: 10.1152/ajpheart.2001.281.3.H1104
23. Takaoka H, Esposito G, Mao L, Suga H, Rockman HA. Heart size-independent analysis of myocardial function in murine pressure overload hypertrophy. *Am J Physiol Heart Circ Physiol*. 2002;282:H2190–H2197. doi: 10.1152/ajpheart.00759.2001
24. Harvey PA, Leinwand LA. The cell biology of disease: cellular mechanisms of cardiomyopathy. *J Cell Biol*. 2011;194:355–365. doi: 10.1083/jcb.201101100
25. Allen DL, Harrison BC, Maass A, Bell ML, Byrnes WC, Leinwand LA. Cardiac and skeletal muscle adaptations to voluntary wheel running in the mouse. *J Appl Physiol (1985)*. 2001;90:1900–1908. doi: 10.1152/jappl.2001.90.5.1900
26. Chung E, Heimiller J, Leinwand LA. Distinct cardiac transcriptional profiles defining pregnancy and exercise. *PLoS One*. 2012;7:e42297. doi: 10.1371/journal.pone.0042297
27. Bernardo BC, Weeks KL, Pretorius L, McMullen JR. Molecular distinction between physiological and pathological cardiac hypertrophy: experimental findings and therapeutic strategies. *Pharmacol Ther*. 2010;128:191–227. doi: 10.1016/j.pharmthera.2010.04.005
28. Martindale JJ, Fernandez R, Thuerauf D, Whittaker R, Gude N, Sussman MA, Glembotski CC. Endoplasmic reticulum stress gene induction and protection from ischemia/reperfusion injury in the hearts of transgenic mice with a tamoxifen-regulated form of ATF6. *Circ Res*. 2006;98:1186–1193. doi: 10.1161/01.RES.0000220643.65941.8d
29. Simpson P. Stimulation of hypertrophy of cultured neonatal rat heart cells through an alpha 1-adrenergic receptor and induction of beating through an alpha 1- and beta 1-adrenergic receptor interaction. Evidence for independent regulation of growth and beating. *Circ Res*. 1985;56:884–894.
30. Basso AD, Mirza A, Liu G, Long BJ, Bishop WR, Kirschmeier P. The farnesyl transferase inhibitor (FTI) SCH66336 (lonafarnib) inhibits Rheb farnesylation and mTOR signaling. Role in FTI enhancement of taxane and tamoxifen anti-tumor activity. *J Biol Chem*. 2005;280:31101–31108. doi: 10.1074/jbc.M503763200
31. Okada K, Minamino T, Tsukamoto Y, et al. Prolonged endoplasmic reticulum stress in hypertrophic and failing heart after aortic constriction: possible contribution of endoplasmic reticulum stress to cardiac myocyte apoptosis. *Circulation*. 2004;110:705–712. doi: 10.1161/01.CIR.0000137836.95625.D4
32. Sari FR, Widyantoro B, Thandavarayan RA, Harima M, Lakshmanan AP, Zhang S, Muslin AJ, Suzuki K, Kodama M, Watanabe K. Attenuation of CHOP-mediated myocardial apoptosis in pressure-overloaded dominant negative p38α mitogen-activated protein kinase mice. *Cell Physiol Biochem*. 2011;27:487–496. doi: 10.1159/000329970
33. Park CS, Cha H, Kwon EJ, Sreenivasaiah PK, Kim DH. The chemical chaperone 4-phenylbutyric acid attenuates pressure-overload cardiac hypertrophy by alleviating endoplasmic reticulum stress. *Biochem Biophys Res Commun*. 2012;421:578–584. doi: 10.1016/j.bbrc.2012.04.048
34. Liu X, Kwak D, Lu Z, Xu X, Fassett J, Wang H, Wei Y, Cavener DR, Hu X, Hall J, Bache RJ, Chen Y. Endoplasmic reticulum stress sensor protein kinase R-like endoplasmic reticulum kinase (PERK) protects against pressure overload-induced heart failure and lung remodeling. *Hypertension*. 2014;64:738–744. doi: 10.1161/HYPERTENSIONAHA.114.03811
35. Vekich JA, Belmont PJ, Thuerauf DJ, Glembotski CC. Protein disulfide isomerase-associated 6 is an ATF6-inducible ER stress response protein that protects cardiac myocytes from ischemia/reperfusion-mediated cell death. *J Mol Cell Cardiol*. 2012;53:259–267. doi: 10.1016/j.yjmcc.2012.05.005
36. Wu J, Ruas JL, Estall JL, Rasbach KA, Choi JH, Ye L, Boström P, Tyra HM, Crawford RW, Campbell KP, Rutkowski DT, Kaufman RJ, Spiegelman BM. The unfolded protein response mediates adaptation to exercise in skeletal muscle through a PGC-1α/ATF6α complex. *Cell Metab*. 2011;13:160–169. doi: 10.1016/j.cmet.2011.01.003
37. Misra J, Kim DK, Choi W, Koo SH, Lee CH, Back SH, Kaufman RJ, Choi HS. Transcriptional cross talk between orphan nuclear receptor ERRγ and transmembrane transcription factor ATF6α coordinates endoplasmic reticulum stress response. *Nucleic Acids Res*. 2013;41:6960–6974. doi: 10.1093/nar/gkt429
38. Tam AB, Roberts LS, Chandra V, Rivera IG, Nomura DK, Forbes DJ, Niwa M. The UPR activator ATF6 responds to proteotoxic and lipotoxic stress by distinct mechanisms. *Dev Cell*. 2018;46:327.e7–343.e7. doi: 10.1016/j.devcel.2018.04.023
39. Yamagata K, Sanders LK, Kaufmann WE, Yee W, Barnes CA, Nathans D, Worley PF. Rheb, a growth factor- and synaptic activity-regulated gene, encodes a novel Ras-related protein. *J Biol Chem*. 1994;269:16333–16339.
40. Potheraveedu VN, Schöpel M, Stoll R, Heumann R. Rheb in neuronal degeneration, regeneration, and connectivity. *Biol Chem*. 2017;398:589–606. doi: 10.1515/hsz-2016-0312
41. Heard JJ, Fong V, Bathaie SZ, Tamanoi F. Recent progress in the study of the Rheb family GTPases. *Cell Signal*. 2014;26:1950–1957. doi: 10.1016/j.cellsig.2014.05.011
42. Goorden SM, Hoogeveen-Westerveld M, Cheng C, van Woerden GM, Mozaffari M, Post L, Duckers HJ, Nellist M, Elgersma Y. Rheb is essential for murine development. *Mol Cell Biol*. 2011;31:1672–1678. doi: 10.1128/MCB.00985-10
43. Wang Y, Huang BP, Luciani DS, Wang X, Johnson JD, Proud CG. Rheb activates protein synthesis and growth in adult rat ventricular cardiomyocytes. *J Mol Cell Cardiol*. 2008;45:812–820. doi: 10.1016/j.yjmcc.2008.07.016
44. Sciarretta S, Zhai P, Shao D, Maejima Y, Robbins J, Volpe M, Condorelli G, Sadoshima J. Rheb is a critical regulator of autophagy during myocardial ischemia: pathophysiological implications in obesity and metabolic syndrome. *Circulation*. 2012;125:1134–1146. doi: 10.1161/CIRCULATIONAHA.111.078212
45. Cao Y, Tao L, Shen S, et al. Cardiac ablation of Rheb1 induces impaired heart growth, endoplasmic reticulum-associated apoptosis and heart failure in infant mice. *Int J Mol Sci*. 2013;14:24380–24398. doi: 10.3390/ijms141224380
46. Schewe DM, Aguirre-Ghiso JA. ATF6alpha-Rheb-mTOR signaling promotes survival of dormant tumor cells in vivo. *Proc Natl Acad Sci USA*. 2008;105:10519–10524. doi: 10.1073/pnas.0800939105
47. Fernandez-Fernandez MR, Ferrer I, Lucas JJ. Impaired ATF6α processing, decreased Rheb and neuronal cell cycle re-entry in Huntington's disease. *Neurobiol Dis*. 2011;41:23–32. doi: 10.1016/j.nbd.2010.08.014
48. Tyagi R, Shahani N, Gorgen L, Ferretti M, Pryor W, Chen PY, Swarnkar S, Worley PF, Karbstein K, Snyder SH, Subramaniam S. Rheb inhibits protein synthesis by activating the PERK-eIF2alpha signaling cascade. *Cell Rep*. 2015;10:684–693. doi: 10.1016/j.celrep.2015.01.014